

Supporting Materials

Text S1 Method for calculating the weight abundance of soil microplastics

Because most of the geotextiles used for reclamation projects covered the surface soil, so the abundance of microplastics in topsoil (upper 2 cm) was taken into consideration. Microplastic load in sediment on a weight basis was calculated based on their size and polymer density (Eqs. (S1)–(S3)). The size of each microplastic was measured and multiplied by a density of 1.04 g/cm³. The shape characteristics of microplastics were simplified to calculate their volumes. Fragment and film types were seen as thin slices cut from a sphere, wherein the volume was multiplied by 0.1, and the fiber type was simplified as a cylinder with a mean diameter detected by the stereomicroscopy (Eo et al., 2019).

$$W_{nf} = 4/3\pi r^3 * \rho * 0.1 \quad , \quad (S1)$$

$$W_f = \pi r^2 h \rho \quad , \quad (S2)$$

$$A = W_t / 0.25kg \quad , \quad (S3)$$

where W_{nf} , W_f , W_t is the weight of non-fiber, fiber and total microplastic particles (g), respectively; r is the radius (μm); h is the measured length of each fiber (μm); ρ is the average polymer density (1.04 g/cm³); A is the weight abundance of microplastic (g/kg); 0.25 kg is the weight of each soil sample.

Text S2 Method for quantifying the soil microplastic weathering situation

Wang et al. (2021) proposed a conditional fragmentation model to describe the size distribution and fragmentation features of soil microplastics. The model parameters and their deduced formula were used to quantitatively evaluate the weathering degree of soil microplastics. The model hypothesized that 1) the driving forces of fragmentation or size reduction of the plastics are natural or artificial factors (e.g., sunlight irradiation, mechanical abrasion, animal activities, etc.) and 2) physical properties such as rigidity and softness of the plastic wastes and debris have less effects on fragmentation or downsizing of the polymers.

$$\lim_{\Delta x \rightarrow 0} \frac{P((x \leq X \leq x + \Delta x) | X > x)}{\Delta x} = a x^b, \quad (S4)$$

where a is a normalization constant and the exponent b or the power law behavior represents a fractal, consistent with the brittle fracturing of particles that results in a branching tree of cracks.

The cumulative distribution function (CDF) deduced from Eq. (S4) can be described by a simple two-parameter model as Eq. (S5):

$$F(x) = 1 - e^{-\lambda x^\alpha} \quad (x \geq 0), \quad (S5)$$

where the parameters $\lambda = a / b + 1$ ($\text{mm}^{-\alpha}$) and $\alpha = b + 1$.

Therefore, the probability density function (PDF) can be expressed as Eq. (S6):

$$f(x) = \lambda \alpha x^{\alpha-1} e^{-\lambda x^\alpha} \quad (x > 0), \quad (S6)$$

Accordingly, this study defined the aging rate as parameter β (mm^{-1}) (Eq. (S7)):

$$\beta = \lambda \alpha x^{\alpha-1}, \quad (S7)$$

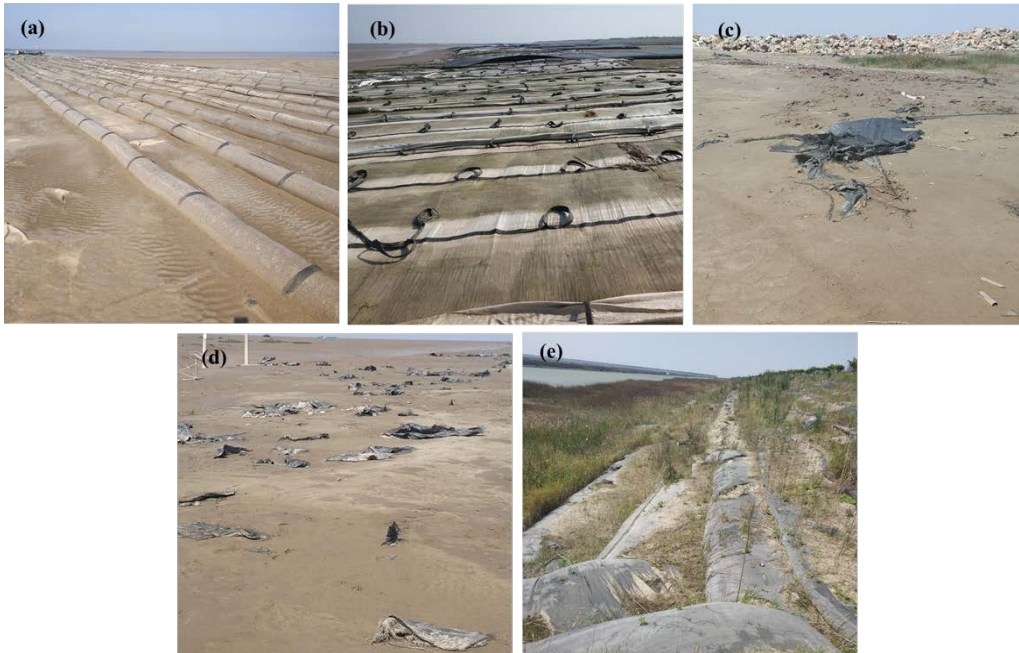


Fig. S1 Images of field survey in reclamation area, (a) S1, (b) S2, (c) S3, (d) S4, (e) S5

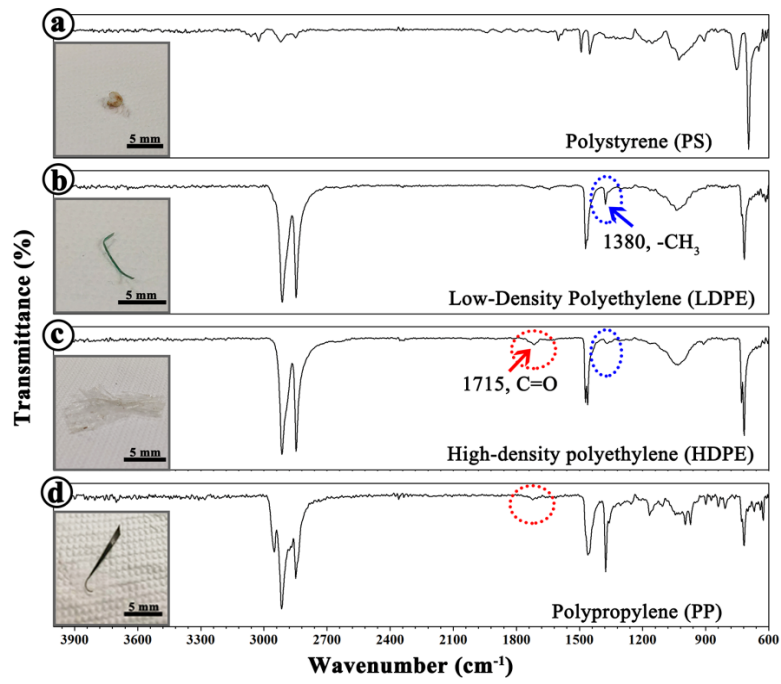


Fig. S2 Identification of soil plastic particles by ATR-FTIR

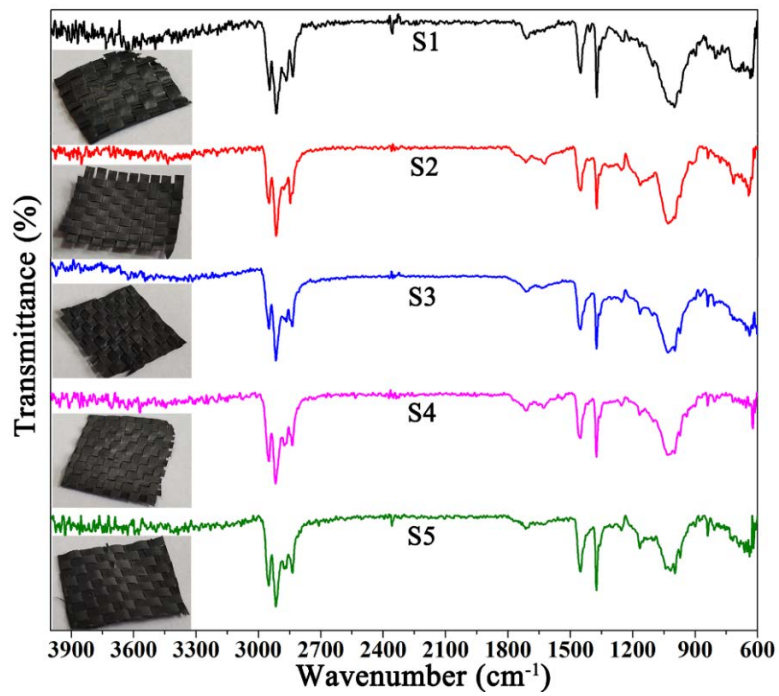


Fig. S3 Identification of weathered geotextile samples by ATR-FTIR

Table S1 Quantitative statistics^{a)} on composition of soil microplastics in shape, color and size (particles/250 g dry weight)

Sampling site	Total amount	Black	Transparent	Red	Blue	Yellow	Green	<100 μm	100–500 μm	500–1000 μm	>1000 μm	Fragment	Fiber	Film
S1	45	20	8	5	6	5	1	16	19	6	4	17	18	10
S2	47	27	3	5	7	4	1	25	14	4	4	28	13	6
S3	63	27	10	10	5	7	4	24	18	11	10	31	29	3
S4	29	10	3	7	4	0	5	7	8	6	8	13	15	1
S5	38	18	5	6	3	3	3	12	19	4	3	24	11	3

Notes: a) The average total amount of each sampling site was statistically analyzed according to the results from stereoscopic microscopy

Table S2 Mean (\pm standard deviation) abundance of soil microplastics (particles/kg dry weight)

Detection method	S1	S2	S3	S4	S5	Mean
Stereoscopic microscopy	167 \pm 20	200 \pm 12	227 \pm 24	135 \pm 26	143 \pm 21	174 \pm 6
Fluorescence microscopy	452 \pm 85	340 \pm 113	412 \pm 266	236 \pm 40	304 \pm 181	349 \pm 137

Table S3 The estimated soil microplastic load under the influence of engineering geotextiles in the reclamation area

Detection method	Units	S1	S2	S3	S4	S5	Mean \pm SD
Stereoscopic microscopy	billion particles	401 \pm 48	480 \pm 29	545 \pm 58	324 \pm 62	343 \pm 50	418 \pm 14
	t	1.58 \pm 0.19	2.28 \pm 0.14	1.94 \pm 0.21	1.35 \pm 0.26	1.61 \pm 0.24	1.75 \pm 0.21
Fluorescence microscopy	billion particles	1085 \pm 204	816 \pm 271	989 \pm 638	566 \pm 96	730 \pm 434	838 \pm 329
	t	4.29 \pm 0.81	3.88 \pm 1.29	3.52 \pm 2.27	2.36 \pm 0.40	3.41 \pm 2.03	3.49 \pm 1.36

Table S4 The abundance of soil microplastics in other published papers, where d.w. stands for dry weight

Location	Sample type	Abundance	Units	Reference
Coast of Dongtai, China	Coastal sand	349 ± 137	Particles/kg d.w.	This study
		12564±4932	Particles/m ²	
Baja California Peninsula, Mexico	Coastal sand	135 ± 92	Particles/kg d.w.	(Pinon-Colin et al., 2018)
North Yellow Sea, China	Coastal sediment	37.1 ± 42.7	Particles/kg d.w.	(Zhu et al., 2018)
Guangdong, China	Coastal sediment	6675 ± 7021	Particles/m ²	(Fok et al., 2017)
Taiwan, China	Coastal sediment	4–532	Particles/12.5 L	(Kunz et al., 2016)
the Republic of Korea	Coastal sand	46334 ± 71291	Particles/m ²	(Kim et al., 2015)
Changjiang Estuary, China	Sediment	121 ± 9	Particles/kg d.w.	(Peng et al., 2017)
Baltic Sea, Russia	Sediment	34 ± 10	Particles/kg d.w.	(Zobkov and Esiukova, 2017)
Bohai Sea, China	Sand	102.9 ± 39.9 to 163.3 ± 37.7	Particles/kg	(Yu et al., 2016)
Poyang Lake, China	Sediment	54–506	Particles/kg d.w.	(Yuan et al., 2019)
Taihu Lake, China	Sediment	11.0–234.6	Particles/kg d.w.	(Su et al., 2016)
Wen-Rui Tang River, China	Sediment	32947 ± 15342	Particles/kg d.w.	(Wang et al., 2018)
Rhine River, Germany	Sediment	228–3763	Particles/kg	(Klein et al., 2015)

References

- Eo S, Hong S H, Song Y K, Han G M, Shim W J (2019). Spatiotemporal distribution and annual load of microplastics in the Nakdong River, Korea. *Water Research*, 160: 228–237 doi:/10.1016/j.watres.2019.05.053
- Fok L, Cheung P K, Tang G D, Li W C (2017). Size distribution of stranded small plastic debris on the coast of Guangdong, South China. *Environmental Pollution*, 220: 407–412 doi:/10.1016/j.envpol.2016.09.079
- Kim I S, Chae D H, Kim S K, Choi S, Woo S B (2015). Factors influencing the spatial variation of microplastics on high-tidal coastal beaches in Korea. *Archives of Environmental Contamination and Toxicology*, 69(3): 299–309 doi:/10.1007/s00244-015-0155-6
- Klein S, Worch E, Knepper T P (2015). Occurrence and spatial distribution of microplastics in river shore sediments of the Rhine-Main area in Germany. *Environmental Science & Technology*, 49(10): 6070–6076 doi:/10.1021/acs.est.5b00492
- Kunz A, Walther B A, Lowemark L, Lee Y C (2016). Distribution and quantity of microplastic on sandy beaches along the northern coast of Taiwan (China). *Marine Pollution Bulletin*, 111(1–2): 126–135 doi:/10.1016/j.marpolbul.2016.07.022
- Peng G Y, Zhu B S, Yang D Q, Su L, Shi H H, Li D J (2017). Microplastics in sediments of the Changjiang Estuary, China. *Environmental Pollution*, 225: 283–290 doi:/10.1016/j.envpol.2016.12.064
- Pinon-Colin T D, Rodriguez-Jimenez R, Pastrana-Corral M A, Rogel-Hernandez E, Wakida F T (2018). Microplastics on sandy beaches of the Baja California Peninsula, Mexico. *Marine Pollution Bulletin*, 131: 63–71 doi:/10.1016/j.marpolbul.2018.03.055
- Su L, Xue Y G, Li L Y, Yang D Q, Kolandhasamy P, Li D J, Shi H H (2016). Microplastics in Taihu Lake, China. *Environmental Pollution*, 216: 711–719 doi:/10.1016/j.envpol.2016.06.036
- Wang L W, Li P F, Zhang Q, Wu W M, Luo J, Hou D Y (2021). Modeling the conditional fragmentation-induced microplastic distribution. *Environmental Science & Technology*, 55(9): 6012–6021 doi:/10.1021/acs.est.1c01042
- Wang Z F, Su B B, Xu X Q, Di D, Huang H, Mei K, Dahlgren R A, Zhang M H, Shang X (2018). Preferential accumulation of small (<300 µm) microplastics in the sediments of a coastal plain river network in eastern China. *Water Research*, 144: 393–401 doi:/10.1016/j.watres.2018.07.050
- Yu X B, Peng J P, Wang J D, Wang K, Bao S W (2016). Occurrence of microplastics in the beach sand of the Chinese inner sea: the Bohai Sea. *Environmental Pollution*, 214: 722–730 doi:/10.1016/j.envpol.2016.04.080
- Yuan W K, Liu X N, Wang W F, Di M X, Wang J (2019). Microplastic abundance, distribution and composition in water, sediments, and wild fish from Poyang Lake, China. *Ecotoxicology and Environmental Safety*, 170: 180–187 doi:/10.1016/j.ecoenv.2018.11.126
- Zhu L, Bai H Y, Chen B J, Sun X M, Qu K M, Xia B (2018). Microplastic pollution in North Yellow Sea, China: Observations on occurrence, distribution and identification. *Science of the Total Environment*, 636: 20–29 doi:/10.1016/j.scitotenv.2018.04.182
- Zobkov M, Esiukova E (2017). Microplastics in Baltic bottom sediments: Quantification procedures and first results. *Marine Pollution Bulletin*, 114(2): 724–732 doi:/10.1016/j.marpolbul.2016.10.060